

A TAXONOMIC REVIEW OF *SUEUS* INFERRED FROM MORPHOLOGICAL AND
MOLECULAR PHYLOGENETIC ANALYSES

By

Matthew Tyler Schiffer

A THESIS

Submitted to
Michigan State University
in partial fulfillment of the requirements
for the degree of

Entomology – Master of Science

2024

ABSTRACT

This research focuses on the ambrosia beetles of the subfamily Scolytinae with a particular emphasis on the *Sueus* genus within the Hyorrhynchini tribe, aiming to clarify their evolutionary history and taxonomic relationships. It employs both morphological and molecular analyses to investigate the phylogenetic relationships within *Sueus*, leading to the identification of a new species and the reevaluation of existing classifications. Specimens for this study were sourced from both international collections and field expeditions across Southeast Asia. The morphological study utilized Leica stereomicroscopes for detailed examinations, while the molecular analysis involved DNA extractions, followed by PCR amplification and sequencing of cytochrome oxidase I (COI) and carbamoyl-phosphate synthetase 2, aspartate transcarbamylase, and dihydroorotase (CAD) genes. This dual approach facilitated the identification of 18 distinct morphological characteristics and unique DNA sequences, enabling the clarification of evolutionary relationships within *Sueus*. The findings include the identification of a new species, *S. insulanus*, the transfer of *S. granulatus* to *Sueus* from *Hyorrhynchus*, and the resurrection of *S. pilosus*. The research underscores the importance of these beetles in forest ecosystems and pest management strategies. It advocates for further studies on the microbiomes of *Sueus*, the potential impacts of climate change on their distribution, and the engagement of citizen science in tracking and managing invasive species.

Copyright by
MATTHEW TYLER SCHIFFER
2024

ACKNOWLEDGEMENTS

I extend my profound gratitude to Dr. Anthony Cognato and Dr. Sarah Smith for their unwavering support and invaluable guidance throughout the development of this research paper and my academic journey as a master's student at Michigan State University. Their insights and encouragement have been pivotal to my growth and achievements. My sincere thanks also go to Dr. Hannah Burrack and the entire team at the MSU Entomology Department for providing me with the opportunity to join this esteemed department and for access to cutting-edge laboratory technology, which has been instrumental in the success of the genetic and molecular studies integral to this research. Their contributions have significantly enriched my educational experience at the university. Additionally, I am deeply appreciative of Dr. Ryan Kimbirauskas for the opportunity to serve as a Teaching Assistant in ISB 201L, a role that has enabled me to develop a better understanding of teaching methodologies and enhance my pedagogical skills. My gratitude also extends to Dr. Amanda Lorenz for offering me enriching experiences in Public Outreach at the Bug House in the Natural Sciences Building. These experiences have broadened my perspective on community engagement and education, allowing me to share my passion for entomology with a wider audience. Moreover, I want to express my heartfelt thanks to Dr. Alan Prather and Dr. Marianna Szucs for serving as members of my Thesis Defense Committee and for their meticulous review of this research before its submission. Together, these individuals have significantly contributed to my personal and professional development, and I am profoundly thankful for their guidance, support, and the opportunities they have provided me during my time at Michigan State University.

In addition, specimens of *S. insulanus* were collected in the framework of "Our Planet Reviewed Papua-New-Guinea 2012-2013" set up by Pro-Natura International, the National Museum of Natural History (MNHN, France), the Institut de Recherche pour le Développement (IRD, France) in partnership with the Royal Belgian Institute of Natural Sciences, the New Guinea Binatang Research Center, the University of Papua New Guinea, and the Divine Word University of Madang and with core funding of Prince Albert II of Monaco Foundation, the

Stavros Niarchos Foundation, the Total Foundation, the Fondation d'entreprise EDF, the Fonds Pacifique, Spiecapag, Entrepose Contracting, the New Caledonia Government, the Reef Foundation, FNRS (Belgium) and the Belgian National Lottery. The IBISCA expert network, the patron for this project, Prof. R.L. Kitching, and all other participants in this collective effort are thanked for their contribution. This study was supported, in part, by a Cooperative Agreement from USDA Forest Service (16-CA-11420004-072 [to A.I.C.]).

TABLE OF CONTENTS

INTRODUCTION.....	1
METHODS & MATERIALS.....	5
RESULTS.....	12
DISCUSSION.....	29
BIBLIOGRAPHY.....	32

INTRODUCTION

Scolytinae, a subfamily within Curculionidae, has traversed the annals of time since the Cretaceous Period, embodying a diverse array of weevils. This subfamily is notably divided into two functional groups—bark beetles and ambrosia beetles—each marked by distinctive features such as reduced snouts, cylindrical bodies, short legs, and antennae, adaptations finely tuned for life within plant tissues (Raffa et al., 2015; Cognato & Grimaldi, 2009).

Functionally classified based on dietary preferences, bark beetles constitute a significant component of Scolytinae. Originally from weevils that consumed leaves, their feeding behaviors now span a spectrum, encompassing species-specific or polyphagous tendencies, targeting leaves, roots, branches, and the phloem of the trunk (Kirkendall et al., 2015). Tree selection is guided by a combination of olfactory and visual cues facilitated by the production of pheromones for both reproduction and aggregation (Rudinsky, 1962; Oliver & Mannion, 2001). Most species target dead, dying, or sick trees, as less than one percent of species regularly colonize healthy trees (Kirkendall et al., 2015).

In contrast, ambrosia beetles form another vital functional group centered around their unique dietary habits. These beetles feed on fungi, transporting fungal spores within specialized cuticular invaginations called mycangium, and can vary drastically in location, shape and size from species to species (Kirkendall et al., 2015). Fungus feeding has independently evolved, fostering relationships ranging from facultative to obligatory symbioses. Each ambrosia beetle species establishes symbiotic connections with specific ambrosia fungi, primarily belonging to the genera *Ambrosiella*, *Rafaellea*, and *Dryadomyces* (Ascomycetes) (Schowalter, 2022).

The life cycle of ambrosia beetles involves the construction of galleries in living or dead plant tissue, where they cultivate carried fungi. The female beetle creates a conducive environment for symbiotic fungal growth and their offspring, inhibiting competing fungi and removing frass. Eggs laid in clusters within the tunnels hatch into larvae that feed on the surrounding fungi, illustrating a complex symbiotic relationship crucial for their survival.

Bark beetles possess physiological and behavioral adaptations that enable them to invade tree tissues effectively. They exhibit resilience to secondary metabolites and the physical and chemical properties of resin, which are typically defensive mechanisms of trees. These beetles can overwhelm host trees by utilizing aggregation pheromones, attracting large numbers of individuals to infest a single tree. The susceptibility of native tree species to invasive bark beetle species also plays a role in their spread, as native trees may have fewer defenses against these invaders (Weed et al., 2015).

Dispersal among these beetles spans a few hundred meters, with occasional long-distance dispersal reaching several kilometers, facilitated by wind currents. Some species within bark and ambrosia beetles, transported through lumber, have become invasive pests, impacting forest ecosystems and agriculture (Oliver & Mannion, 2001). Certain ambrosia beetle species, carrying pathogenic fungi, pose threats to host trees, leading to the weakening and mortality of trees.

With over 6,000 identified species of bark and ambrosia beetles worldwide, accidental introductions into the United States have occurred repeatedly. Between 1984 and 2008, 8,286 exotic beetles were transported via lumber cargo, with 107 species identified (Haack & Rabaglia, 2013). The Neotropics boasts the greatest diversity of scolytine beetles with over 2260 species. The number could be significantly higher due to the limited research conducted in this region (Hulcr et al., 2015).

Various methods are employed to control bark beetle and ambrosia beetle infestations, including the application of pesticides to infected trees to reduce beetle populations. However, once adult females establish galleries and lay eggs within trees, conventional control measures become less effective, as the beetles are protected within the tree's tissues. Attempts to inject pesticides directly into the tree or soil may have limited success in reaching and targeting the beetles. Also, pheromones have been used to deter beetles from infested trees or attract them into traps, aiding population monitoring and control efforts (University of California, 2008). Beyond chemical and pheromone-based approaches, biological control agents play a significant role in managing bark beetle populations. These agents include a variety of native species that naturally

prey upon or parasitize bark beetles, helping to regulate their numbers and limit the extent of infestations.

Many organisms play crucial roles in regulating bark beetle populations by preying on or parasitizing them. Among the most notable predators are woodpeckers and passerine birds, which consume various life stages of bark beetles, contributing to mortality rates of up to 30 percent. Additionally, a diverse array of arthropods, including dipterans, raphidophorans, hemipterans, and other coleopterans, actively prey on bark beetles. Notably, members of Acari (Mites) also play a role in controlling bark beetle populations, although they typically target larvae and pupae rather than adults. These arthropod predators are attracted to bark beetles through chemoreception, responding to compounds emitted by infested trees and aggregation pheromones released by them. In addition to predators, bark beetles face pressure from parasitic organisms. A wide range of endoparasitic and ectoparasitic parasitoids, particularly hymenopterans, target bark beetle populations. Acari and nematodes are also known to parasitize bark beetles, with some nematode species forming mutualistic relationships with their hosts. Furthermore, bark beetles are susceptible to various pathogens, including fungi, bacteria, algae, protists, and viruses. These pathogens can infect bark beetles at different stages of their life cycle, contributing to population control. By targeting bark beetles through predation, parasitism, and infection, these diverse organisms help maintain ecological balance within forest ecosystems and mitigate the impacts of bark beetle outbreaks (Wegensteiner et al., 2015)

Within Scolytinae, the tribe Hyorrhynchini, found in Southeast Asia, stands out. Characterized by well-defined interstriae on the posterior margin of the elytra and an outer margin without socketed teeth, this tribe includes three genera—*Hyorrhynchus*, *Pseudohyorrhynchus*, and *Sueus* (Li et al., 2020; Wood, 1979).

Sueus, a genus within Hyorrhynchini, comprises four species distributed across Southeast Asia and Oceania. *Sueus niisimai* has exhibited a broad geographic distribution, recently identified on the Caribbean Island of Martinique (Smith et al., 2022). These beetles possess distinct traits, such as a female-biased sex ratio, an inbreeding mating system, and haplodiploid genetics, with females being diploid and male's haploid (Beaver & Gebhardt, 2004).

Sueus species create brood galleries in the sapwood of various tree species, cultivating and consuming symbiotic fungi. The pathogenic fungus *Diatrypella japonica* has been identified as the symbiont associated with *S. niisimai* (Li et al., 2020). While specific tree decline has not been linked to this species, concerns arise regarding their potential as pests in agriculture and forestry due to their association with pathogenic fungi, transportability, and mating systems (Rabaglia et al., 2019).

The phylogenetic relationships among *Sueus* species remain unexplored. Given the potential implications for understanding their taxonomy, ecology, and behavior, this study aims to reconstruct phylogenies using morphological and molecular characters. Shedding light on *Sueus* relationships will contribute to our understanding of its potential impact on forest health and pest management.

METHODS & MATERIALS

Sample Collection

Our study used a diverse collection of specimens, including valuable type specimens, from esteemed international entomological repositories such as the Natural History Museum in London, UK (NHMUK), and the Smithsonian National Museum of Natural History in Washington, DC, USA (NMNH). Additionally, we enriched our specimen pool with recently collected samples from field expeditions in Southeast Asia from 2003 to 2023 (Table 1). The three museum specimens were used solely for morphological analysis, and the 24 field-collected specimens were also used in phylogenetic analysis. This comprehensive approach allowed us to leverage the strengths of the museum and freshly collected specimens to conduct a multifaceted investigation.

Our examination focused exclusively on female specimens due to the inherent rarity and infrequency of male ambrosia beetle specimens in entomological collections. These female specimens encompassed all formally described species within the genus. Furthermore, our study incorporated two potential new species and *Hyorrhynchus ebianensis*, which acted as the outgroup for our analysis.

The meticulous specimen identification process was conducted by direct comparison with type specimens (holotypes and syntypes). The specimens were observed using Leica stereomicroscopes, specifically the MZ6 and MZ16 models. The models were illuminated provided by an Ikea Jansjö LED work lamp from Delft, Netherlands. The optical equipment facilitated the precise evaluation of the diagnostic features of these ambrosia beetles. In addition to morphological examinations, we collected quantitative data to determine their distinct characteristics, such as measuring the total length of each specimen from the apex of the pronotum to the apex of the elytra and the width at the broadest point of each specimen.

Species	DNA voucher	Country	State/Province	Locality	Collected from	Date	Collector(s)
<i>S. nisimai</i>	SMS401	Japan	Okinawa	Kunigami District, Yona Experimental Forest		x2011	J. Hulcr
<i>S. pilosus</i>	SMS402	Indonesia	East Java	Jombang: Bangunrejo		18vii2014	A.J. Johnson
<i>S. nisimai</i>	SMS403	Taiwan	Nantou		<i>Machilus</i>	6x2015	A. Black
<i>S. pilosus</i>	SMS404	Vietnam	Vinh Phúc	Tam Dao National Park			M. Jusino
<i>S. nisimai</i>	SMS405	South Korea	Jeju	Jeju Island	<i>Machilus thunbergii</i>		C. Bateman
<i>S. pilosus</i>	SMS406	Thailand	Trang	Khao Bentad Wildlife Sanctuary	Bombacaceae	7x2015	S. Steininger
<i>S. pilosus</i>	SMS407	China	Hong Kong	Tai Po Kau		vi2017	J. Skelton
<i>S. pilosus</i>	SMS408	China	Hainan	Jinping: Qiongzong	<i>Litsea glutinosa</i>	24x2016	Y. Li
<i>S. pilosus</i>	SMS409	China	Guangdong	Guangzhou, SCAU		28x2017	Y. Li
<i>S. nisimai</i>	SMS410	China	Guizhou	Guiyang	<i>Ligustrum</i>	10i2015	Y. Li
<i>S. nisimai</i>	SMS411	China	Jiangxi	Xunwu, Xiangshan		6ix2018	Y. Li
<i>S. nisimai</i>	SMS412	China	Zhejiang	Linan, ZAFU campus		26xii2019	Y. Li
<i>S. nisimai</i>	SMS413	China	Guangxi	Shangsi, Shiwandashan		27iii2018	Y. Li
<i>S. nisimai</i>	SMS414	China	Fujian				Y. Li
<i>S. nisimai</i>	SMS415	Vietnam	Cao Bằng	22°36.454'N 105°52.033'E		15iv2014	A.I. Cognato, S.M. Smith, T.H. Pham
<i>S. pilosus</i>	SMS416	Vietnam	Dong Nia	Cat Tien National Park		22ii2017	A.I. Cognato, T.H. Pham
<i>S. nisimai</i>	SMS417	Vietnam	Ninh Binh	Cuc Phuong National Park			A.I. Cognato, S.M. Smith
<i>S. granulatus</i>	SMS418	Vietnam	Dong Nia	Cat Tien National Park			
<i>S. obesus</i>	SMS419	Thailand	Phetchaburi	Kaeng Krachan N.P., 12.80344N, 99.44015E, 348m		11iv23	S. Smith, W. Sittachaya
<i>S. obesus</i>	SMS420	Thailand	Phetchaburi	Kaeng Krachan N.P., 12.80344N, 99.44015E, 348m	<i>Lithocarpus</i>	11iv23	S. Smith, W. Sittachaya
<i>S. nisimai</i>	SMS421	Vietnam	Thua Thien Hue	Bach Ma National Park		iii2023	A.I. Cognato, P. Gorring
<i>S. insulanus</i>	SMS422	Papua New Guinea	Mt Wilhelm	-5.732514, 145.2568, 700m	Flight Intercept Trap	1-3xi2012	Keltim, Uma, Novotny, Leponce
<i>S. obesus</i>	SMS428	Thailand	Phetchaburi	Kaeng Krachan N.P., 12.80344N, 99.44015E, 348m		11iv23	S. Smith, W. Sittachaya
<i>S. pilosus</i>	SMS429	Martinique	Morne-Rouge	14.75818°N, 61.1242°W, 320 m.		16-30vi2021	F. Deknuydt

Table 1. Geographic and collection data for *Sueus* specimens analyzed in this study.

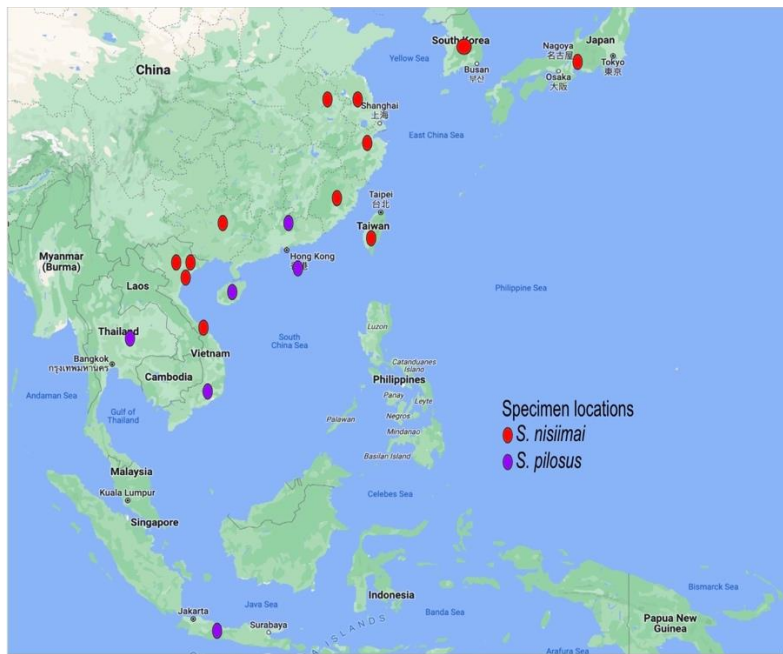


Figure 1. Geographical distribution of *S. nisimai* and *S. pilosus* specimens found within Southeast Asia between 2003–2023.

Morphological Study

For the morphological study, each of the 24 specimens underwent a meticulous examination under magnification to identify phylogenetically informative characters. Characters displaying intraspecific variation were excluded from further analysis. The character states of each character were scored and recorded using the software Mesquite V 3.81 (Maddison & Maddison 2023) (Tables 2 & 3). The resulting morphological dataset was used to construct a phylogenetic tree using a parsimony optimality criterion in PAUP* (Swofford, 2002). We conducted a heuristic search with 30 random additions to explore tree space. We estimated the contribution of character support of the phylogeny with a Jackknife analysis. To assess the robustness of phylogenetic inferences, a jackknife analysis with a 30% deletion was conducted through 100 replicates. The support values for the clades were varied, ranging from 51 to 70.

Character	1	2	3	4	5	6	7	8	9	10	11	12	13	14	15	16	17	18
Taxon																		
<i>H. ebianensis</i>	0	1	0	1	2	0	1	2	3	0	0	0	1	1	3	0	0	0
<i>S. striatulus</i>	0	1	0	1	0	0	0	3	0	1	0	0	0	0	0	1	?	1
<i>S. niisimai</i>	0	0	0	0	0	1	1	0	2	1	1	0	0	0	0	1	0	0
<i>S. insulanus</i>	1	0	1	0	1	0	0	2	1	1	0	1	0	1	2	2	1	0
<i>S. obesus</i>	0	0	1	0	1	1	1	2	1	1	1	0	0	1	1	2	0	1
<i>S. borneensis</i>	0	0	0	0	1	0	0	1	4	1	1	1	1	1	1	1	0	0

Table 2. Character States for Hyorrhynchini Taxa.

Morphological characters and states for Hyorrhynchini taxa.

1. size of pronotum compared to elytra, character index, CI = 1.0

- 0 pronotum smaller than wide
- 1 pronotum larger than wide

2. elytral declivity, CI = 1.0

- 0 obtusely angled
- 1 acutely angled

3. rows of setae in interstriae, CI = 1.0

- 0 1 row of granules
- 1 1-2 rows of asperities

4. setae along elytral declivical margin, CI = 1.0

- 0 absent
- 1 spines along elytral declivity margin

5. episternum setae rows, CI = 1.0
- | | |
|---|---------------------|
| 0 | 3-4 rows of setae |
| 1 | 5 rows of setae |
| 2 | 14-15 rows of setae |
6. ratio of elytral length to elytral width, CI = .500
- | | |
|---|------------------------------|
| 0 | skinny ratio higher than 1.2 |
| 1 | stout ratio lower than 1.2 |
7. percentage of declivity of elytra, CI = .333
- | | |
|---|------------------------|
| 0 | lower than 20 percent |
| 1 | higher than 20 percent |
8. procoxae width, CI = 1.0
- | | |
|---|--------|
| 0 | 1 ou |
| 1 | 2 ou |
| 2 | 1.5 ou |
| 3 | 2.5 ou |
9. ratio of antennal length to antennal width, CI = 1.0
- | | |
|---|---------|
| 0 | .92 ou |
| 1 | 1.25 ou |
| 2 | 1.4 ou |
| 3 | 1.6 ou |
| 4 | 1.87 ou |
10. rows of setae on last abdominal tergite, CI = 1.0
- | | |
|---|-----------|
| 0 | oppressed |
| 1 | straight |
11. length of setae on last abdominal tergite, CI = .500
- | | |
|---|-------|
| 0 | short |
| 1 | long |
12. asperities on last abdominal tergite, CI = .500
- | | |
|---|-------|
| 0 | small |
| 1 | large |
13. number of funicle segments, CI = .500
- | | |
|---|------------|
| 0 | 6 segments |
| 1 | 7 segments |
14. indentation of pronotal suture, CI = .500
- | | |
|---|------|
| 0 | none |
|---|------|

1 present, small

15. length of eyes to median line, CI = 1.0

0 1 ou
1 1.5 ou
2 2 ou
3 4.5 ou

16. setae on frons, CI = 1.0

0 none
1 short
2 long

17. setae below mandibles, CI = 1.0

0 short, spare
1 long, abundant
? unobservable

18. declivity of frons, CI = .500

0 convex
1 concave

DNA extraction, PCR, and sequencing

In the molecular phylogenetic analysis, we focused on specimens of *S. niisimai*, *S. obesus*, two suspected new species, and *Hyorrhynchus* (outgroup). DNA extraction was performed on each specimen's uncrushed head and pronotum separately, following the protocols provided by the Qiagen Tissue DNA extraction kit. After extraction, the head, pronotum, and the remaining body parts were preserved, labeled, and vouchered at the A.J. Cook Arthropod Research Collection.

The purified DNA extracts served as templates for the amplification of specific genetic markers, including portions of cytochrome oxidase I (COI) and cytochrome b (CAD), using the following primer pairs:

- COI - Forward: AACAAATCATAAAGATATTGGRAC, Reverse: GAAATTATNCCAATTCCTGG
- CAD - Forward: TGGAARGARGTBGARTACGARGTGGTYCG, Reverse: GCCATYRCYTCBCCYACRCTYTTTCAT

PCR reactions were prepared with 0.3 μ M of each forward and reverse primer, 1x buffer, 1.75 mM magnesium chloride, 200 μ M dNTPs, 1.25 units of hot star Taq (Qiagen), and approximately 20 ng of DNA template. The PCR program included an initial 15-minute denaturation step (95°C) followed by 38 cycles of 30 seconds denaturation (95°C), 30 seconds annealing (50°C for COI, 55°C for CAD), and 5 minutes extension (72°C). Successful PCR reactions were confirmed by gel electrophoresis using a 1.5% agarose gel stained with ethidium bromide.

Sequencing of PCR products was conducted at the Michigan State University Research Technology Support Facility using BigDye Terminator 1.1 chemistry (Applied Biosystems, Waltham, MA). Forward and reverse sequences were assembled into consensus sequences using Sequencer software. We meticulously examined the sequences for potential anomalies such as pseudogenes and non-*Sueus* DNA.

Phylogenetic Analysis

The verified consensus sequences were compiled into NEXUS files for subsequent phylogenetic analysis using PAUP* 4.0a build 167 (Swofford, 2002) and Mr. Bayes (Ronquist, 2012). In PAUP*, a heuristic search for the most parsimonious trees consisted of 100 repetitions with random stepwise addition via bisection/reconnection. Gaps were treated as missing, and each character was considered unordered and equally weighted. Additionally, we performed a bootstrap analysis of 500 pseudo-replications using a heuristic search with simple stepwise addition. In Mr. Bayes, a phylogenetic tree was constructed based on the mitochondrial gene cytochrome oxidase I (COI) gene, following established protocols used in previous ambrosia beetle studies (Jordal & Cognato, 2012). We employed various search modules to explore tree space and inferred relationships between taxa based on the strict consensus tree. In Mr. Bayes, both the COI and CAD genes underwent partitioning based on codon position, and a model encompassing general time reversal, gamma distribution, and proportion of invariable sites was independently applied to each partition, with parameters not linked between them. The analysis involved running four Metropolis-Coupled Markov Chain Monte Carlo chains, one being the "cold" chain and the other three being "heated" chains. These chains ran simultaneously for 3 million generations, and samples were collected every 100th generation. All model parameters reached a state of stability, and the distribution of splits between the two parallel analyses exhibited a mean standard deviation of 0.0066. To calculate Bayesian posterior probabilities, a

majority-rule consensus tree was generated after discarding the first 25% of saved trees, totaling 45,002 trees. The average estimated sample size for the parameters in the analysis exceeded 100. Percent pairwise DNA difference, measured as p-distance, was computed using PAUP*.

Species concept

Given the shared characteristics between *Sueus* and xyleborine ambrosia beetles, such as female-biased sex ratios, an inbreeding mating system, and haplodiploid genetics, we adopt a consistent species definition. In accordance with established evolutionary lineage hypotheses (Hey 2006, Yeates et al. 2011), we define species as entities marked by their monophyletic taxa, exhibiting discernible characteristics and demonstrating molecular disparities that surpass a predefined threshold indicative of species distinctions within the taxonomic group. In the case of xyleborines, individuals with DNA sequence disparities exceeding 10% for COI and 2% for CAD are recognized as monophyletic and exhibit distinctive morphological traits. These same criteria are now being applied to classify the species within *Sueus*.

RESULTS

Morphological Analysis

The consensus tree resulting from two equally parsimonious trees indicates that *S. obesus* is the sister taxon to *S. granulatus* species, suggesting a potential relationship between these species. Each tree is fully revolved and lacks polytomies. Jackknife analysis assessed the stability of branching patterns within the trees under various character subsets. Notably, the clade containing *S. obesus* and *S. granulatus* showed a support value of 51, indicating relatively lower confidence in this specific relationship.

In the morphological analysis, homoplasy was deduced from the consistency index, with 11 characters having a state of 1.0, six characters showing a state of 0.5, and character 9 (antennal length to width ratio) exhibiting three changes in character states (0.33). Character 9 is diagnostic for *S. niisimai*, character 10 is diagnostic for *S. striatulus*, character 8 is diagnostic for *S. borneensis*, and character 7 is diagnostic for *S. granulatus* and *S. obesus*. There is uncertainty in the 18 employed characters due to high homoplasy of some characters.

A phylogenetic tree was constructed based on 18 morphological characters (Figure 2). However, *S. pilosus* and *S. granulatus* were not included in the analysis. Due to uncertainty surrounding several characters, an additional phylogenetic tree was generated using only five of the least homoplastic characters (3, 4, 10, 11, and 12) (Figure 3).

Morphological analysis of *S. granulatus* and *S. insulanus* revealed distinct characteristics in morphology and genetics, leading to the identification of a new species, the transfer of a *Hyorrhynchus sp.* to *Sueus* and the review of the remaining *Sueus* species.

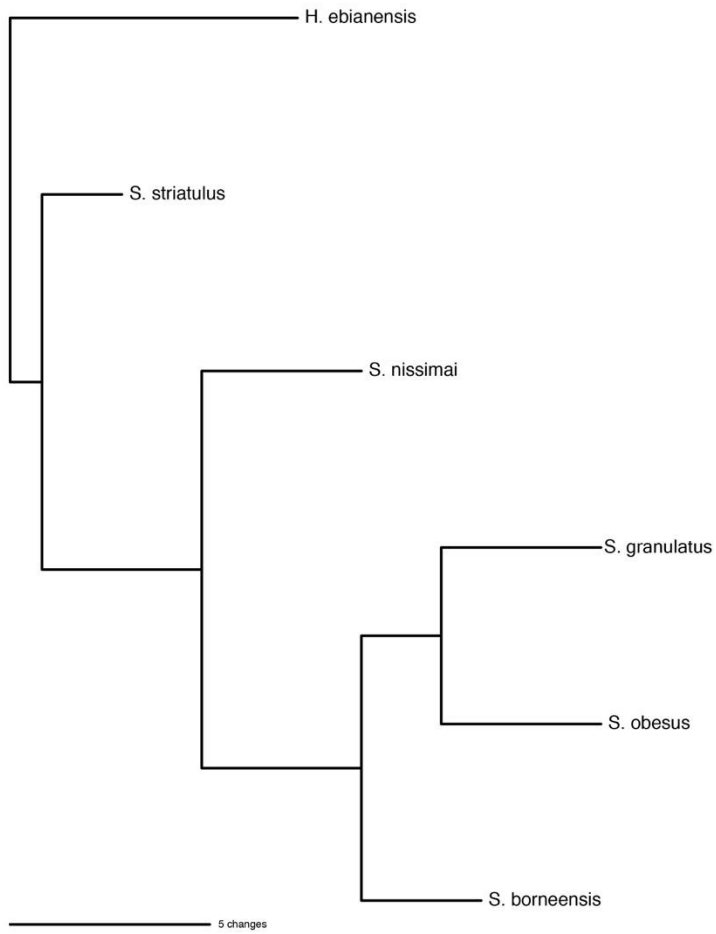


Figure 2. Most parsimonious morphological phylogenetic tree using character 1 to character 18.

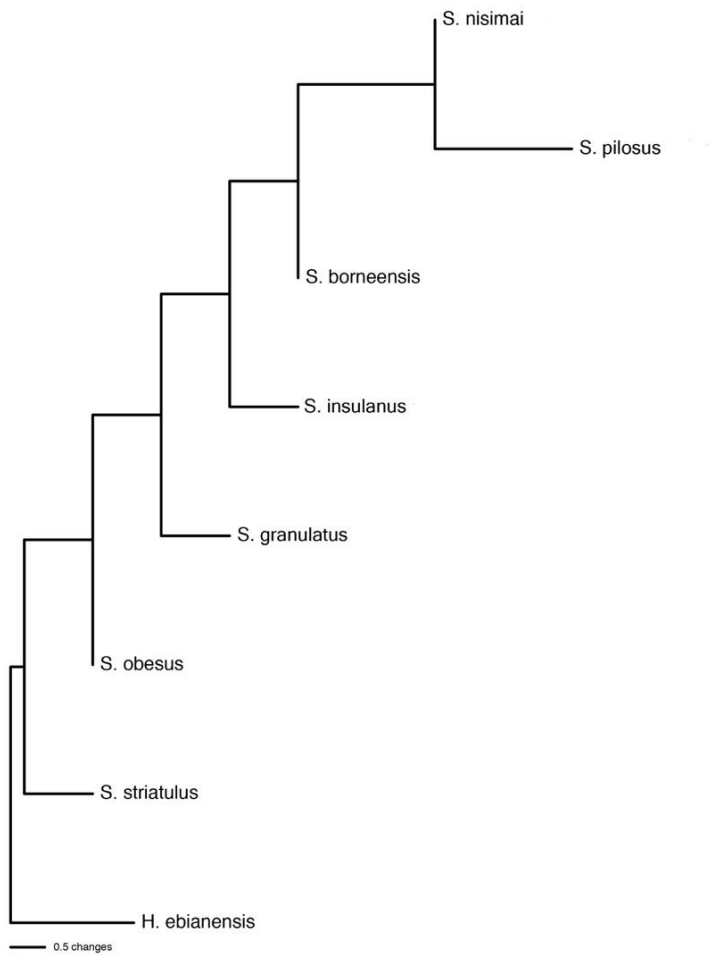


Figure 3. Most parsimonious morphological phylogenetic tree using characters 3,4,10,11, and 12.

Molecular Phylogenetic Analyses

A single, well-resolved parsimonious phylogenetic tree with a length of 875 units was identified (Figure 4). *Sueus nissimai* displayed monophyly, albeit with a bootstrap support of less than 50%. This clade is divided into two subgroups, one closely associated with northern populations (bootstrap = 71%) and the other with southern populations (bootstrap = 99%). Notable morphological distinctions were observed between these subgroups, with individuals in the southern subgroup being identified to be synonymous with *S. pilosus*. Notably, a specimen from Martinique was placed in the southern subgroup of *S. nissimai*.

Sueus obesus exhibited monophyly with a bootstrap value of 100%. *S. granulatus* was found to be sister to the remaining specimens, while the newly discovered species from Papua New Guinea (*S. insulanus* n. sp.) was sister to *S. obesus*.

In the Bayesian analysis, the phylogenetic topology closely resembled the results of the parsimony analysis (refer to Figure 5), albeit with differences in intraspecific resolution and the arrangement of individuals within *S. nissimai* and *S. pilosus*. The posterior probabilities for all species were 1.0 and 0.99 except for the clade comprising *S. nissimai* and *S. pilosus*.

The genetic divergence among conspecifics displayed an average range of approximately 0.00 to 0.01 for the CAD gene and 0.01 to 0.09 for the COI gene (Table 3). Similarly, when considering interspecific comparisons within the *Sueus* species, the genetic variations encompassed a range of 0.00 to 0.06 for CAD and 0.16 to 0.22 for COI, respectively. These results are typical species boundaries for haplodiploid xyleborines.

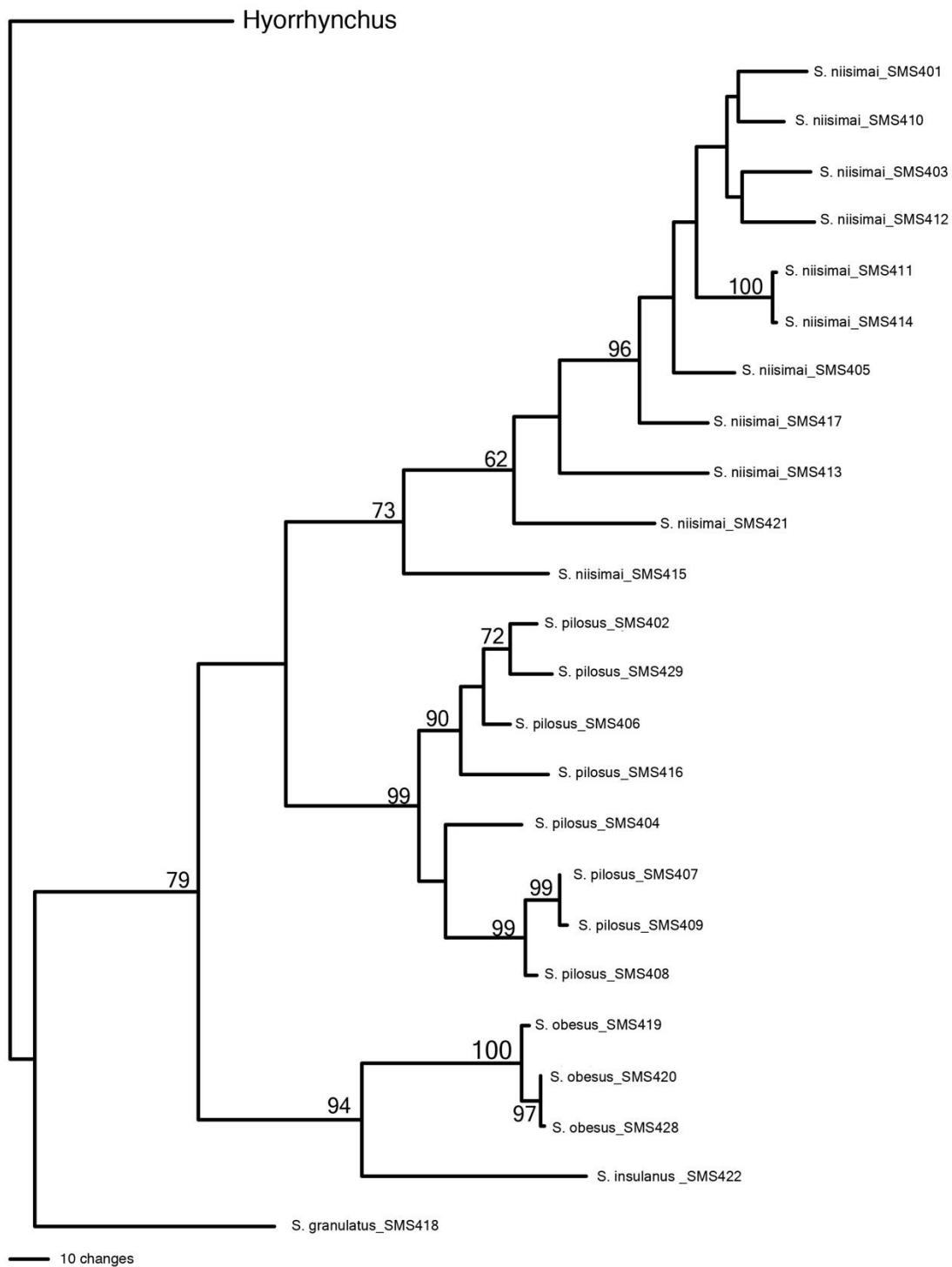


Figure 4. NA-based phylogeny inferred from parsimony analysis (COI and CAD Genes). The robustness of the phylogenetic relationships is assessed through bootstrap values associated with each clade. The bootstrap values of each clade ranged from 62 to 100.

Intraspecific mean and range	<i>S. niisimai</i> (0.01; 0.02- 0.00)	<i>S. pilosus</i> (0.01; 0.01 - 0.00)	<i>S. obesus</i> (0.00; 0.00 - 0.00)	<i>S. insulanus</i> (-)	<i>S. granulatus</i> (-)
<i>S. niisimai</i> (0.09; 0.15 - 0.00)	-	0.02; (0.03 - 0.01)	0.06; (0.07-0.06)	0.00; (0.00-0.00)	0.05; 0.05-0.04
<i>S. pilosus</i> (0.06; 0.09 - 0.02)	0.17; (0.19-0.14)	-	0.06; (0.06 -0.06)	0.00; (0.00-0.00)	0.04; 0.05-0.04
<i>S. obesus</i> (0.01; 0.01 - 0.00)	0.18; (0.19-0.16)	0.17; (0.18-0.15)	-	0.00; (0.00-0.00)	0.00; (0.00-0.00)
<i>S. insulanus</i> (-)	0.20; (0.21-0.17)	0.19; (0.21-0.19)	0.16; (0.16 - 0.16)	-	0.00; (0.00-0.00)
<i>S. granulatus</i> (-)	0.20; (0.21-0.19)	0.17; (0.19-0.04)	0.16, (0.16 - 0.16)	0.22; (0.22-0.22)	-

Table 3. Mean (range) p - distances for pairwise comparisons of *Sueus* species. Top diagonal = CAD; bottom diagonal = COI.

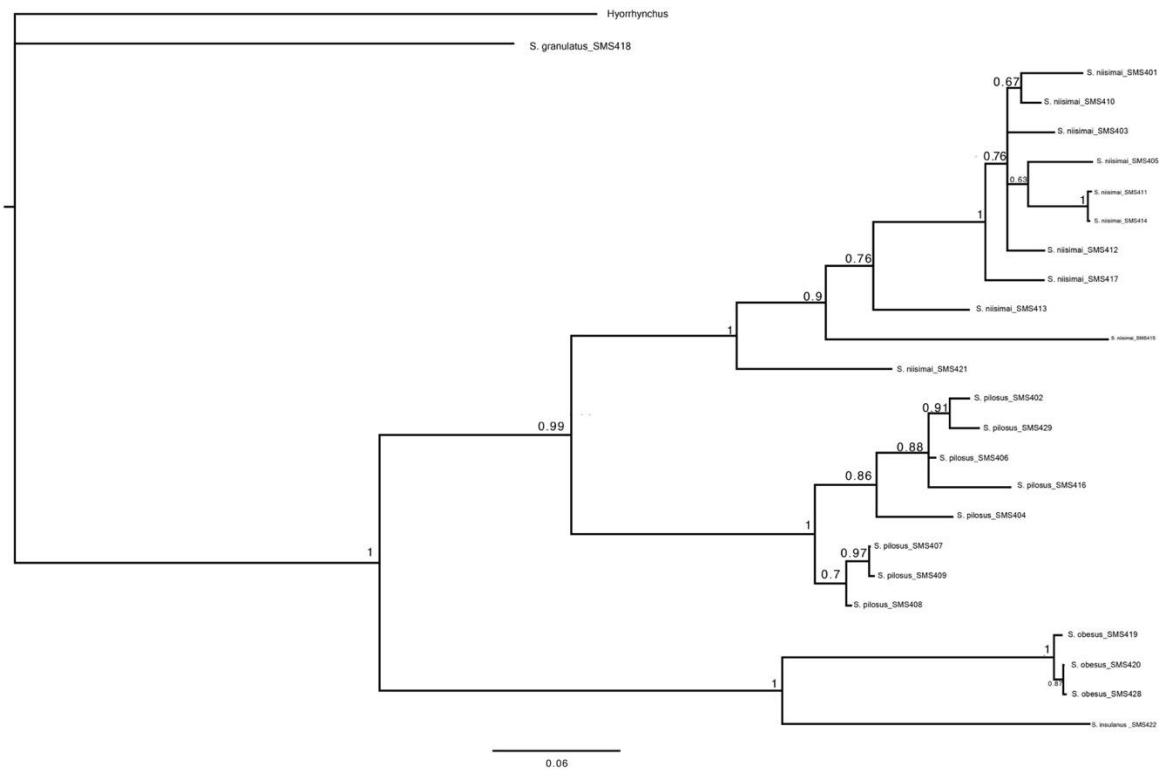


Figure 5. DNA-based phylogeny inferred from Bayesian Analysis.

Bayesian analysis depicting the phylogenetic relationships among various taxa based on COI and CAD sequences. The length of each branch equals the number of nucleotide changes and are not time calibrated.

Taxonomy

Sueus Murayama 1951

Sueus Murayama 1951: 1. Type species *Sueus sphaerotrypoides* Murayama 1951 = *Hyorrhynchus niisimai* Eggers, 1926.

Diagnosis. A combination of characters including: completely divided eyes without a separating carina, slightly flatten conical antennal club that is less then 1.5x longer then wide, six or seven segmented antennal funicle (female), outer apical angle of the protibia produced into one conspicuous spine, widely separated procoxae, and dwarf males distinguishes *Sueus* from other scolytines and Hyorrhynchini genera, *Hyorrhynchus* and *Pseudohyorrhynchus*. These two genera have completely divided eyes separated, in part, by a carina (males), flatten antennal club that is 1.5 to 2.0x longer then wide, and seven segmented antennal funicle, and male sizes that are comparable to females.

Sueus borneensis Bright, 1994

(Fig. 6)

Sueus borneensis Bright, 1994: 271.

Type Specimen. Holotype, examined.

Other specimens examined.

New records.

Diagnosis. No more than two rows of interstitial setae and weakly impressed striae distinguish this species from the other *Sueus* species. **Host.** Various- likely mycetophagous.

Distribution Borneo.

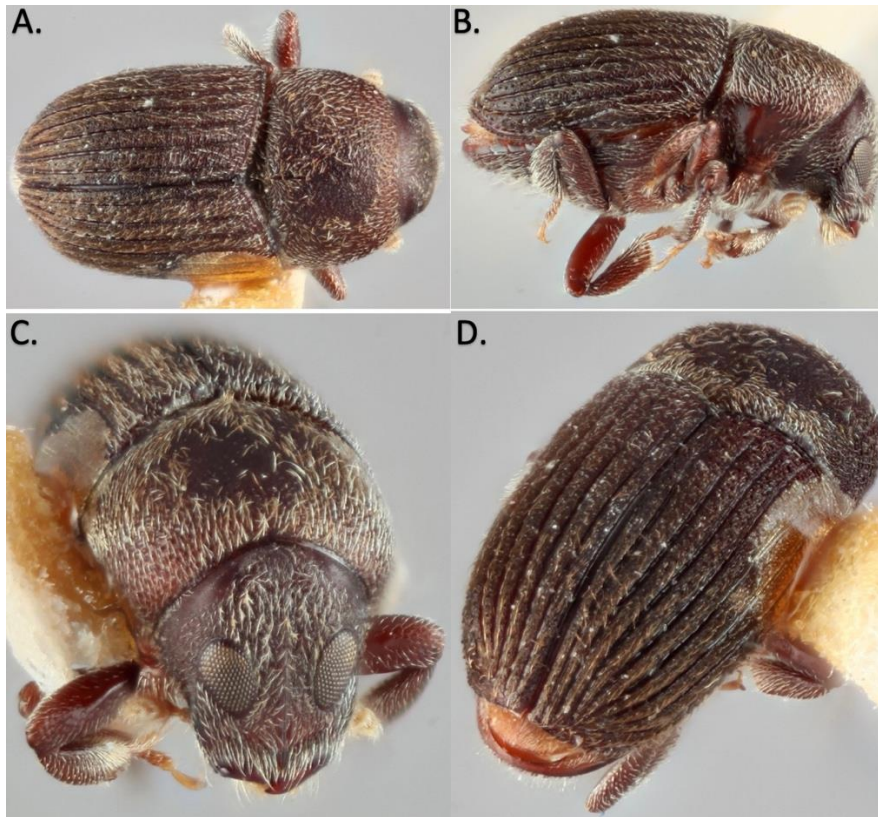


Figure 6. *Sueus borneensis*, dorsal, lateral, frontal, and posterior view (A,B,C,D).

Sueus niisimai (Eggers, 1926)

(Fig. 7)

Hyorrhynchus niisimai Eggers, 1926: 133.

Sueus niisimai (Eggers):

Sphaerotrypes controversa Murayama 1950: 62

Sueus sphaerotrypoides Murayama 1951a: 2

Type Specimen. Syntype, examined.

Other specimens examined. See Table 1

Diagnosis. The longer main setae and the short ground vesiture (< width of interstria) on the elytral declivity distinguish this species from the other *Sueus* species.

Host. Various- likely mycetophagous.

Distribution. Found throughout eastern Asia including China, Japan, South Korea, Taiwan, and northern Vietnam. It is possibility distributed more northerly as compared to *S. pilosus*. Also there are records from Australia, Fiji (introduced), Malaysia, Sri Lanka, and Papua New Guinea (Beaver 1983, Beaver and Gebhardt 2004, Li et al. 2020) which need verification given potential misidentification with the more southernly distributed *S. pilosus*.



Figure 7. A syntype of *Sueus niisimai*, dorsal, lateral, frontal, and posterior view (A,B,C,D).

Sueus obesus (Browne, 1977)

(Fig. 8)

Hyorrhynchus obesus Browne, 1977: 369

Sueus obesus (Browne): Beaver and Gebhardt, 2004: 96

Type Specimen. Holotype, NHMUK, examined.

Other specimens examined. see Table 1.

Diagnosis. No more than two rows of interstrial setae and strongly impressed striae distinguish this species from the other *Sueus* species.

Host. Various- likely mycetophagous.

Distribution. Thailand and Malaysia.

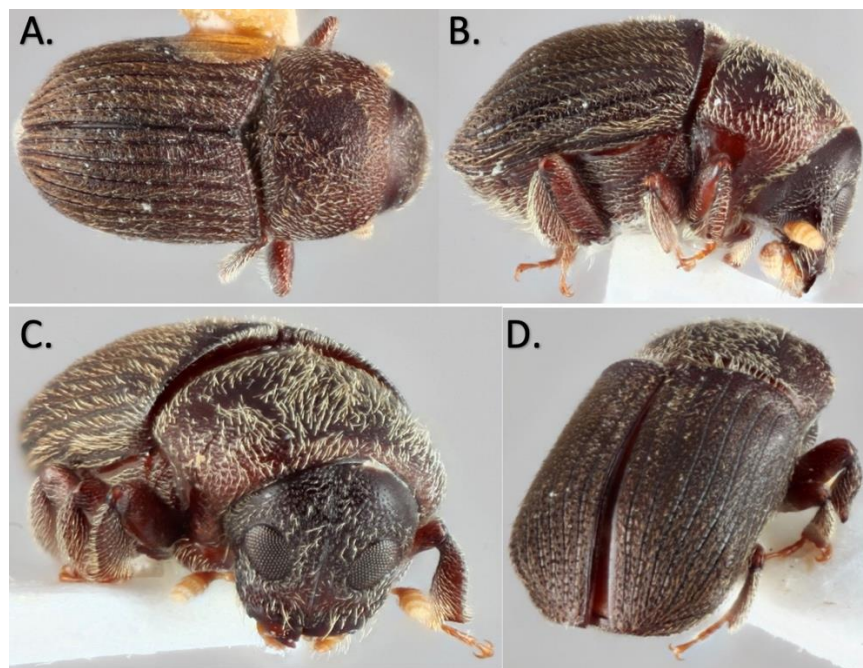


Figure 8. *Sueus obesus*, dorsal, lateral, frontal and posterior view (A,B,C,D).

Sueus pilosus (Eggers, 1936), stat. res.

(Fig. 9)

Hyorrhynchus pilosus Eggers, 1936: 81.

Type Specimen. Paratype (NMNH), examined.

Other specimens examined. See Table 1.

New records. Laos: Bolikhamxai Prov. 18°21'N, 105°08'E, Nape (8 km NE), ~600m, Vit Kubán leg.; Hua Phan Prov. 20°12'N, 104°01'E, Phu Phan Mt., ~1750m, 17v-3vi2007, Vit Kubán leg.; Phongsaly Prov., 21°41'N, 102°6'E, Phongsaly env., 6-17v2004, ~1500m, Vit Kubán leg. **Sumatra:** G. Sinngalang, S of Bukittinggi. 14-16ii1991, 1300m. Bocák & Bocákováłgt.

Diagnosis. The similar size of the main setae and the long ground vestiture (> width of interstria) on the elytral declivity distinguish this species from the other *Sueus* species.

Host. Various- likely mycetophagous.

Distribution. Occurring in southern China, Thailand, southern Vietnam and Indonesia possibility distributed more southernly as compared to *S. niisimai*. Introduced to Martinique.

Remarks. Schedl (1962: 202) placed *S. pilosus* in synonymy with *S. niisimai* without an explicit reason. Reciprocal monophyly, greater than 10% COI nucleotide difference, and morphological diagnostic characters support the restored status of *S. pilosus*.



Figure 9. Holotype of *Sueus pilosus*, dorsal, lateral, frontal and posterior view (A,B,C,D).

Sueus striatulus (Schedl, 1954)

(Fig. 10)

Hyorrhynchus striatulus Schedl, 1954: 145.

Neohyorrhynchus striatulus (Schedl): Schedl 1962: 202.

Sueus striatulus (Schedl): Wood 1983: 650.

Type Specimen. Holotype, examined.

Diagnosis. The smaller size (~1.5 mm) and granules on the elytral apical margin distinguishes this species from the other *Sueus* species.

Host. Unknown- likely mycetophagous.

Distribution. Likely Java .

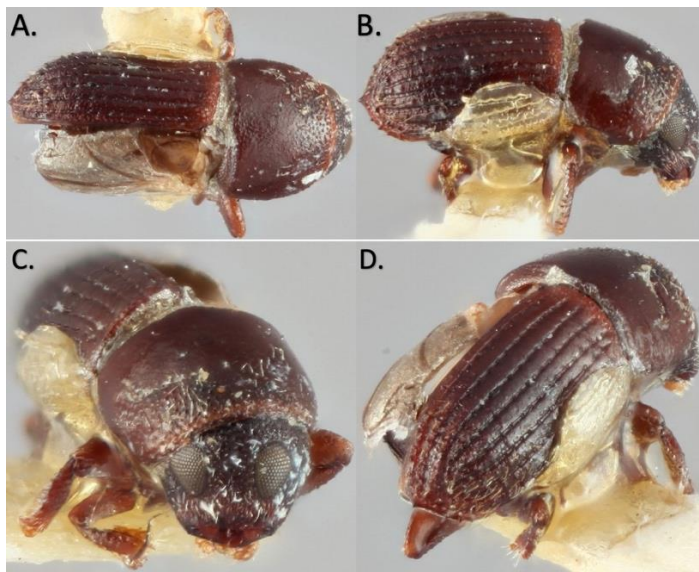


Figure 10. The holotype of *Sueus striatulus*, dorsal, lateral, frontal and posterior view (A,B,C,D).

Sueus insulanus, new species

(Fig. 11)

Type material. Holotype, female, DNA Voucher SMS422, Papua New Guinea: Mt Wilhelm, -5.731961, 145.2522, 700m, Coll. by Keltim, Uma, Novotny, Leponce; P1237 Plot 18, FIT-MW700-R-4/8-d08, 1/11/[20]12 -3/11/[20]12; DNA Voucher SMS422 (MSUC). Papua New Guinea: Mt Wilhelm, -5.739897, 145.3297, 200m, Coll. by Dilu, Ray, Novotny, Leponce; P0802 Plot 12, FIT-MW200-L-7/8-d14, 7/11/[20]12 -9/11/[20]12 (MNHN). Each specimen includes the label, “Our Planet Reviewed –MNHN/PNI/IRD 2012”.

Diagnosis. The appressed setae the interstriae of the elytral declivity distinguishes this species from the other *Sueus* species.

Description. Female: Length 2.2-2.4 mm, about 2.0 times longer than wide. Frons weakly convex, with a distinct, sharply elevated, longitudinal carina extending from epistomal margin to upper level of eyes; surface dull, densely and finely punctate-granulate, with fine, golden-brown setae. Antennal funicle 5-segmented; club conical slightly flattened, with 3 transverse sutures. Pronotum 1.6 times wider than long, widest slightly behind middle; lateral margin evenly arcuate, more strongly converging on anterior half; surface densely, finely granulate and weakly punctate, with scattered, long, golden-brown setae. Elytra 1.4 times longer than wide; sides weakly arcuate, apex narrowly rounded; discal striae very narrow, shining, lightly impressed, more strongly impressed toward declivity, striae punctures fine, shallow; discal interstriae much wider than striae, granulate, with long, fine, appressed, golden-brown setae. Declivity convex; surface as on disc except striae distinctly more deeply impressed, interstriae slightly narrower, fewer granules. Third tarsal segment entire.

Host. Unknown- likely mycetophagous.

Distribution. Papua New Guinea

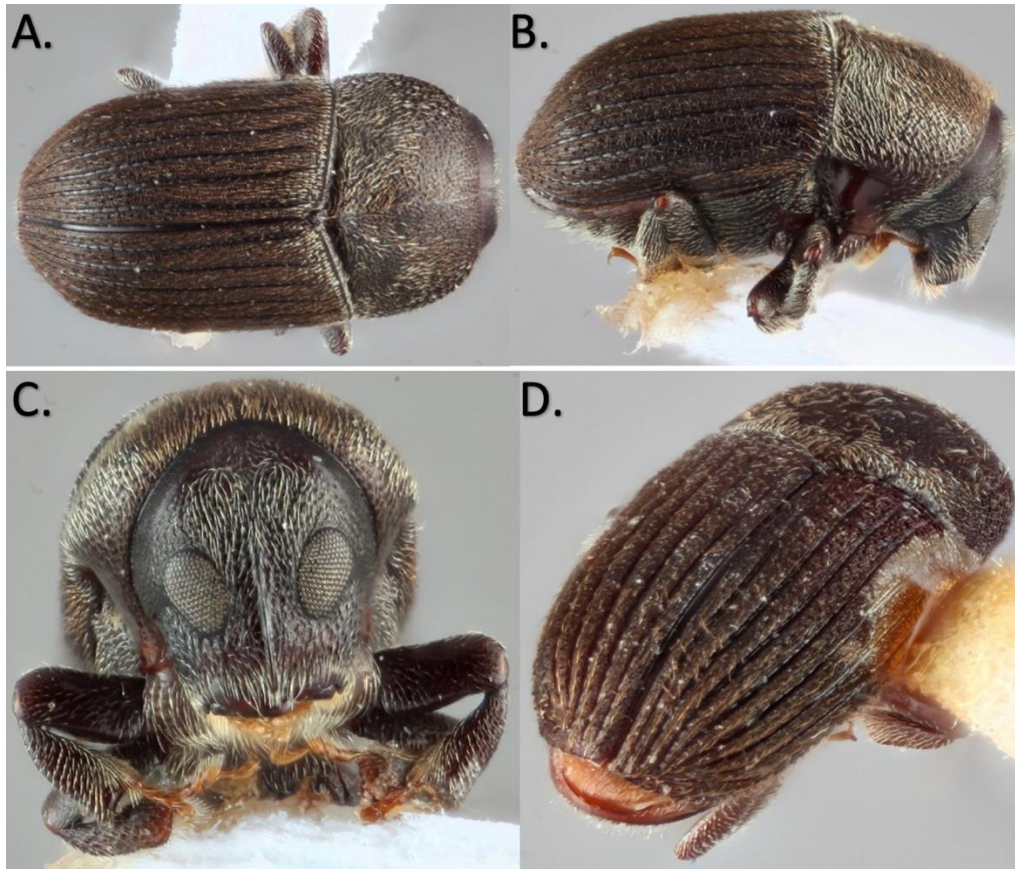


Figure 11. The holotype of *Sueus insulanus*, dorsal, lateral, frontal and posterior view (A,B,C,D).

***Sueus granulatus*, (Eggers), stat. res., new combination**

(Fig. 12)

Hyorrhynchus granulatus Eggers, 1936: 80

Type material. Holotype, female, NHMW, photo examined.

New records. Vietnam: Dong Nai Prov. Cat Tien NP, 11.42232, 107.42834, 128 m. 25iii2017. AI Cognato, TA Hong. ex. 1-3 cm dia. branch. (# MSUC)

Diagnosis. The larger size (~3 mm) and granules comprising the interstriae of the elytral declivity distinguishes this species from the other *Sueus* species.

Host. Unknown- likely mycetophagous.

Distribution. Java, Vietnam

Remarks. Wood and Bright (1992) attributed the synonymy of *H. granulatus* and *H. drescheri* Eggers, 1936 with *H. lewisi* Blandford, 1894 to Schedl (1962). However, this was a misinterpretation of Schedl's (1962), generic grouping of these species. Inspection of images of both type specimens revealed that the granulate elytral declivity is only diagnostic for *H. granulatus*. As with Beaver and Liu (2010) and M. Knižek (in Beaver and Liu 2010), we recognize this dissimilarity, and we remove *H. granulatus* from synonymy with *H. lewisi*. Furthermore, generic level diagnostic characters, especially the shape of the antennal club, are consistent with those of *Sueus*.



Figure 12. *Sueus granulatus*, dorsal, lateral, frontal and posterior view (A,B,C,D).

Dichotomous key

1. Granules on the interstriae of the elytral declivital face:
 - Large, visible above setae in lateral profile: *S. granulatus*
 - Small, hidden by setae in lateral profile: Go to 2
2. Granules on the elytral apical margin:
 - Present: *S. striatulus*
 - Absent: Go to 3
3. Number of rows of interstitial setae:
 - 1 or 2: Go to 4
 - 3 or 4: Go to 5
4. Impression elytra strial:
 - Strongly impressed: *S. obesus*
 - Weakly impressed: *S. borneensis*
5. Elytral interstitial setae and body size:
 - Appressed and larger (~2.5mm): *S. insulanus*
 - Erected and smaller (~1.6mm): Go to 6
6. Elytral interstitial setae:
 - Main setae and ground vestiture similar sizes; ground vestiture longer than width of interstria: *S. pilosus*
 - Main setae longer than ground vestiture; ground vestiture shorter than width of interstria: *S. niisimai*

DISCUSSION

Phylogenetic analysis of morphological and DNA datasets allowed for the reassessment of *Sueus* species relationships. The topologies of the morphological and molecular phylogenies differed except for the sister relationship of *S. niisimai* and *S. pilosus*. Support values for the morphologically based tree were low compared to the DNA based phylogenies which was likely due to the inclusion of only a few parsimony informative characters (Figure 2). The inclusion of morphological and molecular characters into a combined phylogenetic analysis may have helped to increase phylogenetic support like in other studies however, it was not feasible due to the lack of concordance of taxa between datasets. Although the species relationships based on the morphological phylogenetic analysis were tenuous, the analysis provided insight into diagnostic characters used for the recognition of species. The new species exhibited morphological differences consistent with the differences observed in other species, such as the state of the elytral declivital setae and corresponding long branch lengths in the DNA-based phylogenies. These extended branches suggest a lack of diversity within these taxa or an early separation from other related taxa. As seen in other xyleborines, *Sueus* species engage in inbreeding with their siblings during reproduction. This reproductive strategy may contribute to an intense founder effect, where only a few females are required to establish a new population, further influencing the observed long branches in the phylogeny. This divergence may also indicate that these species carry unknown species of pathogenic fungi. The DNA divergence of *S. insulanus* was comparable to other species. Its placement sister to *S. obesus* in the DNA-based phylogenies was well supported but given the long branch lengths an alternative sister species relationship may be possible (Figure 4). As for the other species, the sister position of *S. granulatus* to all other *Sueus* species gives credence to its previous generic placement in *Hyorrhynchus* however, the morphological diagnostic character of the antennal club is clearly of *Sueus*. An expanded phylogenetic analysis including more *Hyorrhynchus* species will test the generic placement of *S. granulatus*.

Most illuminating was the discovery of phylogenetic structure among individuals of the widespread *S. niisimai*. Assumed to occur throughout eastern Asia, Indonesia and Oceania, we demonstrated that *S. niisimai* comprised two main clades separated by a mean of 17% COI DNA divergence. These clades are associated with diagnostic morphology – short ground vestiture versus long ground vestiture. Also, the clades roughly correspond to geographic location- *S.*

niisimai in the north and *S. pilosus* in the south (Figure 1). The intraspecific COI divergence of some *S. niisimai* individuals ranged beyond the 10% approximated for species boundaries as with other inbred scolytines with female biased sex ratios, however, the intraspecific CAD divergence remained below 2% within hypothetical species boundaries (Cognato et al. 2020). The lineages represented by individuals SMS413, SMS415, and SMS421 may represent cryptic or psuedocryptic species given that obvious morphological differences were not observed (Smith and Cognato 2022).

In addition, we demonstrated that the *S. niisimai* discovered in the Caribbean is *S. pilosus* (Smith et al. 2022). It is unknown if the presence of *S. pilosus* in Martinique is due to a prehistoric dispersal and/or contemporary human mediated dispersal as observed with other ambrosia beetles (Golhi et al. 2016, Rabaglia et al. 2019). The DNA-based phylogeny suggests that the *S. pilosus* from Martinique is closely related to *S. pilosus* from East Java. An Asian/Neotropical relationship between populations of widespread ambrosia beetles have been observed (Golhi et al. 2016, Urvois et al. 2023). Given that the similarity of the Martinique and East Java COI DNA sequences are not near zero (divergence = 2.6%), there is the potential that the Martinique specimen was sourced from another location in southeast Asia. Additional sampling of *S. pilosus* throughout Indonesia and southeast Asia is needed to confidently determine the origins of the Martinique *S. pilosus*.

Future investigations

Future investigations into *Sueus* should expand the sampling of specimens from each species. Excluding *S. niisimai* and *S. pilosus*, the specimen collection for each studied species was limited. Expanding the collection to include more specimens would enhance our understanding of the distribution and host tree specificity of these ambrosia beetles. Incorporating a broader array of specimens into the phylogenetic analysis could encompass all currently recognized species within the *Sueus* genus. Such an expansion would not only refine our understanding of the phylogenetic relationships within the tribe Hyorrhynchini but also shed light on the historical dispersal and evolutionary dynamics of this genus. Gathering more *S. niisimai* specimens from various populations might also uncover the existence of additional cryptic species. Furthermore, integrating specimens from related genera such as *Hyorrhynchus* and *Pseudohyorrhynchus* could necessitate taxonomic revisions and possibly lead to species

being reclassified. The presence of an *S. niisimai* specimen from Martinique suggests the insects' expansion beyond their initial habitat, necessitating further research to trace the trajectory and source of this invasion. Subsequent studies would benefit from including specimens from *S. borneensis* and *S. striatulus* for a more comprehensive phylogenetic understanding of the *Sueus* genus.

BIBLIOGRAPHY

- Cambronero-Heinrichs, J. C., Battisti, A., Biedermann, P. H., Cavaletto, G., Castro-Gutierrez, V., Favaro, L., Santolemma, G., & Rassati, D. 2023.** Erwiniaceae bacteria play defensive and nutritional roles in two widespread ambrosia beetles. *FEMS Microbiology Ecology*, 99(12).
- Cognato, A. I., and J-H. Sun. 2007.** DNA based cladograms augment the discovery of a new *Ips* species from China (Coleoptera: Curculionidae: Scolytinae). *Cladistics*, 23: 539–551. doi.org/10.1111/j.1096-0031.2007.00159.x.
- Beaver, R. A., & Gebhardt, H. 2004.** Notes on the tribe Hyorrhynchini (Col. Curculionidae, Scolytinae). *Serangga*, 9: 91-102.
- Beaver, R. A. 1984.** Biology of the Ambrosia Beetle, *Sueus niisimai* (Eggers) (Coleoptera: Scolytidae), in Fiji. *Entomologists' Monthly Magazine*, 120: 99–102.
- Beaver, R. A., Sittichaya, W., & Liu, L. Y. 2014.** A synopsis of the scolytine ambrosia beetles of Thailand (Coleoptera: Curculionidae: Scolytinae). *Zootaxa*, 3875 (1): 1-82.
- Blandford W. F. H. 1894.** The Rhynchophorous Coleoptera of Japan. Part III. Scolytidae. *Transactions of the Entomological Society of London* 1894, 53–141.
- Cognato, A. I., & Grimaldi, D. 2009.** 100 million years of morphological conservatism in bark beetles (Coleoptera: Curculionidae: Scolytinae). *Systematic Entomology*, 34: 93-100.
- Eggers H. (1936).** Neue indomalayische Borkenkäfer (Ipidae) III Nachtrag. *Tijdschrift voor Entomologie*, 79: 77–91.
- Haack, R. A., Rabaglia, R. J., & Peña, J. E. (2013).** Exotic bark and ambrosia beetles in the USA: potential and current invaders. *Potential invasive pests of agricultural crops*. CAB International, Wallingford, 48-74.
- Hulcr, J., Atkinson, T. H., Cognato, A. I., Jordal, B. H., & McKenna, D. D. 2015.** Morphology, taxonomy, and phylogenetics of bark beetles. In *Bark Beetles*. Academic Press, 41-84.
- Jordal, B., & Cognato, A. 2012.** Molecular phylogeny of bark beetles reveals multiple origins of fungus farming during periods of global warming. *BMC Evolutionary Biology*, 12: 133. (doi:10.1186/1471-2148-12-133) <https://doi.org/10.1186/1471-2148-12-133>.
- Kirkendall, L., Biedermann, P., & Jordal, B. 2015.** Evolution and Diversity of Bark and Ambrosia Beetles. (doi:10.1016/B978-0-12-417156-5.00003-4) <https://doi.org/10.1016/B978-0-12-417156-5.00003-4>.
- Li, Y., Skelton, J., Adams, S., Hattori, Y., Smith, M. E., & Hulcr, J. 2020.** The Ambrosia Beetle *Sueus niisimai* (Scolytinae: Hyorrhynchini) is Associated with the Canker Disease Fungus *Diatrypella japonica* (Xylariales). *Plant Disease*, 104(12), 3143–3150. (doi.org/10.1094/PDIS-03-20-0482-RE) <https://doi.org/10.1094/PDIS-03-20-0482-RE>.

- Maddison, W. P., & Maddison, D. R. 2023.** Mesquite: a modular system for evolutionary analysis. Version 3.81. (<http://www.mesquiteproject.org>)(<http://www.mesquiteproject.org>).
- Oliver, J. B., & Mannion, C. M. 2001.** Ambrosia beetle (Coleoptera: Scolytidae) species attacking chestnut and captured in ethanol-baited traps in middle Tennessee. *Environmental Entomology*, 30 (5): 909-918.
- Rabaglia, R. J., Cognato, A. I., Hoebeke, E. R., Johnson, C. W., Labonte, J. R., Carter, M. E., & Vlach, J. J. 2019.** Early detection and rapid response: a 10-year summary of the USDA Forest Service program of surveillance for non-native bark and ambrosia beetles. *American Entomologist*, 65: 29–42.
- Raffa, K., Grégoire, J.-C., & Lindgren, B. S. 2015.** Natural History and Ecology of Bark Beetles. (doi:10.1016/B978-0-12-417156-5.00001-0) <https://doi.org/10.1016/B978-0-12-417156-5.00001-0>.
- Ronquist, F., Teslenko, M., van der Mark, P., Ayres, D. L., Darling, A., Höhna, S., Larget, B., Liu, L., Suchard, M. A., & Huelsenbeck, J. P. 2012.** MrBayes 3.2: efficient Bayesian phylogenetic inference and model choice across a large model space. *Systematic Biology*, 61(3), 539–542. (doi.org/10.1093/sysbio/sys029)(<https://doi.org/10.1093/sysbio/sys029>).
- Rudinsky, J. A. 1962.** Ecology of Scolytidae. *Annual Review of Entomology*, 7 (1): 327-348.
- Schedl, K. E. 1954.** Fauna indomalayensis IV. 141 Beitrag zur Morphologie und Systematik der Scolytoidea. *Philippine Journal of Science*, 83: 137 - 159.
- Schowalter, T. D. 2022.** Chapter 8—Species interactions. In T. D. Schowalter (Ed.), *Insect Ecology* (Fifth Edition). Academic Press, 349–409, (doi.org/10.1016/B978-0-323-85673-7.00002-2) <https://doi.org/10.1016/B978-0-323-85673-7.00002-2>.
- Seybold, S. J., Paine, T. D., & Dreistadt, S. H. 2008.** (University of California Statewide IPM Program). University of California. <https://ipm.ucanr.edu/PMG/PESTNOTES/pn7421.html>.
- Smith, S., Touroult, J., & Cognato, A. 2022.** The First Report of *Sueus niisimai* (Eggers, 1923) (Coleoptera: Curculionidae: Scolytinae: Hyorrhynchini) from the Western Hemisphere, from the Caribbean Island of Martinique. *The Coleopterists Bulletin*, 76 (3): 364-366.
- Swofford, D. 2002.** PAUP. Phylogenetic Analysis Using Parsimony (and Other Methods). Version 4.0b10. (doi:10.1111/j.0014-3820.2002.tb00191.x) <https://ipm.ucanr.edu/PMG/PESTNOTES/pn7421.html>.
- Wegensteiner, R., Wermelinger, B., Herrmann, M. 2015.** Chapter 7 - Natural Enemies of Bark Beetles: Predators, Parasitoids, Pathogens, and Nematodes, Academic Press, 247-304, ISBN 9780124171565, <https://doi.org/10.1016/B978-0-12-417156-5.00007-1>.
- Weed, A.S., Ayres, M.P., Bentz, B.J. 2015.** Chapter 4 - Population Dynamics of Bark Beetles, Editor(s): Fernando E. Vega, Richard W. Hofstetter, *Bark Beetles*, Academic Press, 157-176, ISBN 9780124171565, <https://doi.org/10.1016/B978-0-12-417156-5.00004-6>.